A Finite-State Fixed-Corridor Model for UAS Traffic Management

Hossein Rastgoftar[®], Member, IEEE, Hamid Emadi, and Ella M. Atkins[®], Senior Member, IEEE

Abstract—This paper proposes a fluid-flow-inspired solution for low altitude Uncrewed Aircraft System (UAS) Traffic Management (UTM) in urban areas. We decompose UTM into spatial and temporal planning problems. For the spatial planning problem, we use the principles of Eulerian continuum mechanics to safely and optimally allocate airspace to a UAS. To this end, the finite airspace is partitioned into keep-in and keep-out subspaces with keep-out subspace(s) or zone(s) enclosing buildings and restricted no-fly regions. The keep-in subspace is divided into navigable channels that safely wrap keep-out zone(s). We define the airspace planning problem with a Dynamic Programming (DP) formulation in which states are defined based on spatial and temporal airspace features and actions denote transitions between safe navigable channels. We apply the proposed traffic management solution to enable safe coordination of multiple small UAS at low-altitude airspace populated with buildings of varied footprints and heights.

Index Terms—UAS traffic management (UTM), Markov decision process (MDP), path planning.

I. INTRODUCTION

NCREWED Aircraft Systems (UAS) were originally developed for military applications [1]. UAS are also becoming popular in a variety of industrial and academic research applications due to benefits such as their agility, low operational cost, and ability to observe and transit through a complex three-dimensional environment. UAS applications include small package delivery [2], data acquisition from hazardous environments [3], agricultural inspection and chemical application [4], aerial surveillance [5], urban search and rescue [6], wildlife monitoring and exploration [7] and urban traffic monitoring [8].

To safely integrate UAS into low altitude airspace, the Federal Aviation Administration (FAA) has published rules that restrict or prohibit UAS operators from flying near sensitive regions like airports, stadiums or prisons. UAS must also remain clear of conventional aircraft airspace corridors, terrain,

Manuscript received 11 April 2022; revised 25 July 2023 and 26 September 2023; accepted 28 September 2023. Date of publication 29 November 2023; date of current version 18 April 2024. This work was supported by the National Science Foundation under Award 2133690 and Award 1914581. The Associate Editor for this article was S. Rathinam. (Corresponding author: Hossein Rastgoftar.)

Hossein Rastgoftar is with the Department of Aerospace and Mechanical Engineering (AME) and the Department of Electrical and Computer Engineering (ECE), The University of Arizona, Tucson, AZ 19085 USA (e-mail: hrastgoftar@arizona.edu).

Hamid Emadi was with the Aerospace and Mechanical Engineering (AME), University of Arizona, Tucson, AZ 19085 USA (e-mail: hamidemadi@arizona.edu).

Ella M. Atkins is with Department of Aerospace and Ocean Engineering, Virginia Tech, Blacksburg, VA 24061 USA (e-mail: ematkins@vt.edu). Digital Object Identifier 10.1109/TITS.2023.3324250

and infrastructure. A UAS traffic management (UTM) system inspired by manned air traffic management (ATM) [9] has been proposed to manage UAS traffic in low-altitude airspace. UTM has to-date focused on defining a sparse and static set of UAS traffic corridors, but these manually-defined and mapped corridors will significantly limit transiting UAS traffic density and throughput. Moreover, UTM requires a transition to autonomy and datalink that will no longer support see-and-avoid and voice-based single-UAS traffic coordination. The UTM framework must therefore include protocols to assure traffic coordination and collision avoidance along with support for high-density, high-throughput operations. This paper describes a planning strategy to support collision-free UAS transit through high-density airspace. Related work to UAS and a paper overview are provided below.

A. Related Work

UTM development by the National Aeronautics and Space Administration (NASA) and FAA is summarized in [10], [11], and [12]. In particular, NASA and FAA are developing UTM-specific metrics and protocols to authenticate users, manage datalink and databases, separate UAS from manned aircraft, and provide updated information to users. A candidate UTM concept of operations in [13] discusses the roles and responsibilities of UTM and UAS pilots. Although the approach in [13] is fundamentally based on manned air traffic control, relevant methods of UAS control, maneuverability, range, and operational constraints are presented. Sunil et al. [14] compare airspace safety and capacity with different protocols ranging from free-flight to a network of fixed corridors with preplanned UAS trajectories meeting separation standards. Issues in deploying UTM for autonomous point-to-point UAS traffic are discussed in [15].

A primary UTM challenge is to assure operational scalability [16], particularly for payload transport applications. This has led package transport companies to propose service models of UTM [17], e.g., low-speed local traffic, high-speed transit layer traffic. Authors in [18] propose a first-come-first-serve procedure to avoid trajectory conflicts. Because UTM will blanket the ground with low-altitude UAS, UTM protocols must also responsibly integrate with a diverse suite of overflown communities mapped by property zoning, a mobile population, navigation signal availability, terrain, manmade infrastructure, and community preferences [19].

A three-dimensional air corridor system is proposed in [20] to safely manage low-altitude UAS traffic. Zhai et al. [21] present a computationally efficient global subdivision method

1558-0016 © 2023 IEEE. Personal use is permitted, but republication/redistribution requires IEEE permission. See https://www.ieee.org/publications/rights/index.html for more information.

to organize traffic. Four types of low-altitude air routes are designed with a discrete grid transforming the complex spatial computation problem into a spatial database query. Airspace geofencing has been proposed to assure UAS respect no-flyzones and remain within their allocated airspace volumes [22], [23], [24]. Kim and Atkins [25] present three-dimensional flight volumization algorithms using computational geometry and offers path planning solutions responsive to dynamic airspace allocation constraints. Graph search methods such as A* [26] and D* [27] can efficiently generate solutions with abstract or local-area search spaces. Roadmaps such as Voronoi and visibility graphs and random sampling approaches [28] such as RRT* [29] reduce search space complexity in 2-D and 3-D environments.

Researchers have developed different methods for UAS coordination. For example, containment control [30], consensus-based control [31], partial differential-based approach [32], graph-based methods [33] and continuum deformation approach [34], [35]. The Control Barrier Function (CBF) approach can be used for ensuring the safety of multi-UAS coordination [38]. CBF is commonly defined for control affine systems by choosing a Lipschitz continuous control that ensures *forward invariance* over a specified safety zone [39], [40]. Vascik et al. [41] propose a geometric aerospace assessment based on seven operational features.

Available multi-agent coordination methods such as consensus, containment control, and continuum deformation pressume the total number of agents is fixed in a given motion space. In emerging multi-agent coordination applications, such as Unmanned Aerial System (UAS) Traffic Management (UTM), where UAS can freely enter or leave the airspace and the airspace's capacity is time-varying, this assumption must be relaxed. Therefore, we adopt a Eulerian continuum mechanics model for UAS coordination in this paper. Our model considers UAS as particles of ideal fluid flow sliding along the streamlines of the flow pattern. By imposing wall boundary conditions on the external boundaries of urban obstacles, we ensure collision avoidance while maximizing airspace usability by enabling UAS to safely pass through this constrained environment.

B. Contributions and Outline

This paper proposes defining UAS traffic coordination for UTM as a spatiotemporal planning problem. For spatial planning, we define UAS trajectories along the streamlines produced by the ideal fluid flow patterns, therefore, UAS coordination is governed by the Laplace partial differential equation (PDE) with inspiration from [35] which can ensure collision avoidance with stationary obstacles and failed UAS. Terrain, buildings, and infrastructure are wrapped by airspace obstacles (i.e., no-fly zones) through which we propose the design of fixed airway corridors. In particular, we divide the airspace into different layers and assign each UAS to transit in a fixed altitude layer along that layer's prescribed traffic flow streamline. Transitions between air corridor layers are permitted at a cost that encourages each UAS to remain in a single layer when possible. For temporal planning, we define a dynamic program (DP) to authorize safe UAS transitions between air corridors in a centralized manner consistent with current concepts proposed for community-based UTM. Compared to the existing literature and the authors' previous work [35], [36], [37] this paper offers the following novel contributions:

- We propose a UTM architecture that includes time-invariant air corridor layers for transiting UAS traffic. Specifically, obstacle-free air corridor geometries are defined by solving a Laplace PDE that safely wraps buildings and no-flight-zones at low computation cost,
- We propose a DP-based collision-free multi-vehicle path planning strategy that applies a first-come-first-serve prioritization to UAS airway corridor allocation.
- 3) Compared to the CBF approach [39], [40], [42], [43] that can ensure safety given *forward invariance* for control of affine systems, we propose a novel model-free collision avoidance method that treats each obstacle as a "rigid body" whose boundary is determined by a streamline enclosing it. Therefore, boundaries enclosing obstacles are not trespassed when desired UAS trajectories are defined along the streamlines generated by solving a Laplace PDE over an obstacle-laden motion space.

The remainder of this paper is organized as follows. Section II provides a problem statement followed by a description of our methodology in Section III. The operation of the proposed layered UTM airspace is summarized in Section IV. Simulation results are presented in Section V followed by a brief conclusion in Section VI.

II. PROBLEM STATEMENT

This paper develops a fluid-flow-inspired UTM solution to maximize safe low-altitude airspace occupancy by small UAS. Our proposed solution defines UAS routing as a spatiotemporal planning problem. For spatial planning, UAS coordination is defined by an ideal fluid flow pattern with potential and stream functions obtained by solving Laplace PDEs [35], [44]. This solution offers the following advantages:

- The streamlines define the boundaries of air corridors that safely wrap building and no-fly-zones in lowaltitude airspace.
- 2) The system can be solved in real-time to guarantee collision avoidance given UAS failures and dynamic evolution of local airspace no-fly zone geometry.

For temporal planning, we apply a DP formulation to manage UAS coordination by optimally allocating air corridors to UAS according to a first-come-first-serve prioritization. This work makes the following simplifying assumption.

Assumption 1: Airspace corridor design and allocation is centralized. Each UAS is connected to a single local UTM cloud computing system managing low-altitude airspace for that region.

III. METHODOLOGY

This section presents a mathematical framework for UAS path planning for different tasks in a 3-D obstacle-laden environment. To this end, we first define fixed air corridors by treating UAS coordination as ideal fluid flow that safely wraps keep-out airspace in Section III-A. Then, we define

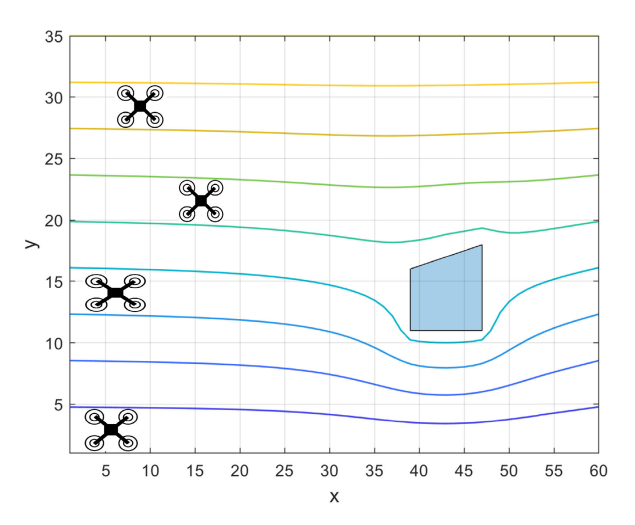


Fig. 1. Streamlines in the x - y plane for an environment with a polygonal obstacle

a DP with constrained actions specifying possible transitions between and along air corridors. We use the Bellman equation to obtain the optimal policy over the full DP state space. As a result, we can optimally allocate air corridors to the UAS requesting passage through the managed airspace volume.

A. Spatial Planning: Air Corridor Generation Using Fluid Flow Navigation

First, we present the foundations of ideal fluid flow coordination. Second, we discuss how fluid flow coordination can be applied to generate safe air corridors in urban low-altitude airspace.

1) Ideal Fluid Flow Pattern: In this work, we treat UAS as particles in an ideal flow moving on streamlines that wrap keep-out airspace zones. Here, the keep-out zones represent buildings and restricted flight areas [35] (See Fig. 1). The lowaltitude airspace is represented by a finite number of parallel planes (floors), each of which is normal to the z axis and lying on the x-y plane, as shown in Fig. 1. A floor is denoted by $\mathcal{C} \subset \mathbb{R}^2$ and divided into keep-in and keep-out regions, where keep-out zones are projection of buildings and obstacles on the floor.

Suppose a floor C contains n_o keep-out zones defined by disjoint closed sets of $\mathcal{O}_1, \ldots, \mathcal{O}_{n_o}$, and use complex variable $\mathbf{z} = x + \mathbf{i} y$ to denote position over the floor C. By defining UAS coordination as an ideal fluid flow pattern over compact set $C \subset \mathbb{R}^2$, we can obtain potential function $\Phi(x, y)$ and stream function $\Psi(x, y)$ of the ideal fluid flow field by defining a conformal mapping

$$f(\mathbf{z}) = \Phi(x, y) + \mathbf{i}\Psi(x, y), \qquad (1)$$

with $\Phi(x, y)$ and $\Psi(x, y)$ that satisfy the Laplace PDE and Cauchy-Riemann conditions

$$\nabla^2 \Psi = 0, \quad \nabla^2 \Phi = 0, \tag{2}$$

$$\frac{\partial \Phi}{\partial x} = \frac{\partial \Psi}{\partial y}, \quad \frac{\partial \Phi}{\partial y} = -\frac{\partial \Psi}{\partial x}.$$
 (3)

Using the ideal fluid flow model [35], x and y components of the ith UAS are constrained to slide along stream curve Ψ_i defined as follows:

$$\Psi_i \triangleq \Psi(x_i(t_0), y_i(t_0)), \tag{4}$$

where $x_i(t_0)$ and $y_i(t_0)$ are x and y components of the ith UAS position at reference time t_0 when it enters C through a boundary point. We can use analytic and numerical approaches to define $\Phi(x, y)$ and $\Psi(x, y)$ over C as described next.

a) Analytic solution: keep-out or "no-fly" airspace zones defined by $\mathcal{O}_1, \ldots, \mathcal{O}_{n_o}$ can be safely wrapped by defining Φ and Ψ as the real and imaginary parts of complex function

$$f(\mathbf{z}) = \sum_{i=1}^{n_o} \left(\mathbf{z} - \mathbf{z}_i + \frac{r_i^2}{\mathbf{z} - \mathbf{z}_i} \right), \tag{5}$$

where $\mathbf{z}_i = x_i + \mathbf{j}y_i$ and $r_i > 0$ denote the nominal position and size of the *i*-th keep-out zone, respectively. Here, r_i must be sufficiently large so that the *i*-th obstacle, a polygon in \mathcal{C} , is safely enclosed by the closed domain generated by analytic function f defined by Eq. (5).

Remark 1: For $n_o = 1$, a single compact keep-out region existing in C is wrapped by a circle of radius r_i with center positioned at \mathbf{z}_i . However, when $n_o > 1$, keep-out zones are not wrapped with a circular area. Therefore, analytic solution (5) cannot be used for environments containing arbitrary obstacles.

b) Numerical solution: When environments contains obstacles with arbitrary non-circular sections, we use the finite difference approach to determine Φ or Ψ values over the motion space. The finite-difference method discretizes the governing PDE and the environment by replacing the partial derivatives with their approximations. We therefore uniformly discretize \mathcal{C} into small regions with increments in the x and y directions given as Δx and Δy , respectively. We use graph $\mathcal{G}(\mathcal{V},\mathcal{E})$ to uniformly discretize \mathcal{C} where $\mathcal{V} = \{1,\ldots,m\}$ and $\mathcal{E} \subseteq \mathcal{V} \times \mathcal{V}$ define nodes and edges of \mathcal{G} , respectively.

We express set $\mathcal{V} = \{1, \dots, m\}$ as $\mathcal{V} = \mathcal{V}_B \bigcup \mathcal{V}_I \bigcup \mathcal{V}_O$ where disjoint sets $\mathcal{V}_B = \{1, \dots, m_B\}, \mathcal{V}_I = \{m_B+1, \dots, m_B+m_I\}$, and $\mathcal{V}_O = \{m_B+m_I+1, \dots, m\}$ identify boundary, interior, and obstacle nodes, respectively (i.e. $m = |\mathcal{V}|$ is the total number of nodes used for discretization of \mathcal{C}). Fig. 4 shows a uniform discretization of rectangular domain \mathcal{C} with the boundaries denoted by $\partial \mathcal{C}_1$, $\partial \mathcal{C}_3$, $\partial \mathcal{C}_2$, and $\partial \mathcal{C}_4$.

Assuming the UAS objective is to safely move from left to right, we impose the following conditions (constraints) on Ψ over V_B and V_O :

$$\Psi(j) = \begin{cases} y_j & j \in \partial \mathcal{C}_2 \bigcup \partial \mathcal{C}_4 \\ x_j & j \in \partial \mathcal{C}_1 \bigcup \partial \mathcal{C}_3 \end{cases}$$
 (6)

Assuming n_o (compact) obstacles exist, obstacles are identified by set $\mathcal{M} = \{1, \dots, n_o\}$, and \mathcal{V}_O can be expressed as

$$\mathcal{V}_O = \bigcup_{j=\mathcal{M}} \mathcal{U}_j \tag{7}$$

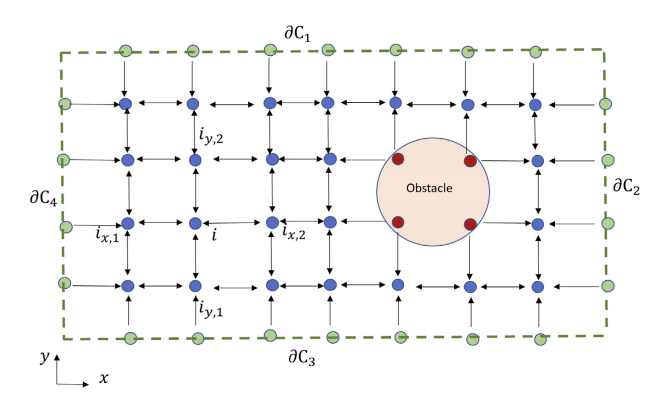


Fig. 2. Directed graph \mathcal{G} discretizes the x-y plane. Green, blue and red nodes correspond respectively to the boundary, feasible space and single circular obstacle.

where U_j defines all the nodes contained by the *j*-th obstacle. For obstacle $j \in \mathcal{M}$, we define

$$\bar{x}_j = \frac{\sum_{i \in \mathcal{U}_j} x_i}{|\mathcal{U}_j|}, \quad j \in \mathcal{M},$$
 (8a)

$$\bar{y}_j = \frac{\sum_{i \in \mathcal{U}_j} y_i}{|\mathcal{U}_i|}, \quad j \in \mathcal{M},$$
(8b)

as the nominal position of obstacle $j \in \mathcal{M}$. Then, the stream values of the obstacle nodes are defined by

$$\Psi(i) = \bar{y}_j, \quad i \in \mathcal{U}_j, \ j \in \mathcal{M}. \tag{9}$$

By substituting the approximated derivatives from the Taylor series to (2), stream value function Ψ_i at node $i \in \mathcal{V}_I$ satisfies the following equation:

$$\frac{\Psi_{i_{x,1}} - 2\Psi_i + \Psi_{i_{x,2}}}{\Lambda x^2} + \frac{\Psi_{i_{y,1}} - 2\Psi_i + \Psi_{i_{y,2}}}{\Lambda y^2} = 0, \quad (10)$$

where $\Psi_{i_{x,1}}$ and $\Psi_{i_{x,2}}$ are Ψ values at the neighbor nodes in the x direction, i.e. $(i_{x,1},i)$, $(i_{x,2},i) \in \mathcal{E}$. Similarly, $\Psi_{i_{y,1}}$ and $\Psi_{i_{y,2}}$ are the Ψ values at the neighbor nodes in the y direction, i.e. $(i_{y,1},i)$, $(i_{y,2},i) \in \mathcal{E}$.

By defining $\Psi = [\Psi_1 \dots \Psi_m]^T$ as the vector aggregating nodal stream values, Eq. (10) can then be written in compact form

$$\mathbf{L}\Psi = \mathbf{0} \tag{11}$$

where $\mathbf{L} = [L_{ij}] \in \mathbb{R}^{m \times m}$ is the Laplacian matrix of graph \mathcal{G} with (i, j) entry

$$L_{ij} = \begin{cases} \deg(i) & i = j \\ -1 & i \neq j, (i, j) \in \mathcal{E} \\ 0 & \text{otherwise.} \end{cases}$$
 (12)

In Eq. (12), $\deg(i)$ is the in-degree of node i. According to [45] the multiplicity of eigenvalue 0 of \mathbf{L} is equal to the number of maximal reachable vertex sets. In other words, multiplicity of zero eigenvalues is the number of trees needed to cover graph \mathcal{G} . Therefore, matrix \mathbf{L} has $m_B + m_O$ eigenvalues equal to 0. Hence, the rank of L is $m - m_B + m_O$.

Let $\bar{\Psi} = \left[\Psi_{m_B+1}, \dots, \Psi_{m_B+m_I}\right]$ denote the vector of Ψ values corresponding to the interior nodes. Since rank of \mathbf{L} is $m - m_B + m_O$, Eq. (11) can be solved for $\bar{\Psi}$. Details of this numerical approach are presented in [35]. Fig. 1 shows the streamlines in a rectangular environment wrapping a polygonal obstacle obtained with the numerical approach presented above.

- 2) Air Corridor Separation: To ensure collision avoidance between every two UAS, we impose the following two requirements:
 - 1) **Requirement 1:** The desired path of every UAS is defined along a streamline. Therefore, the desired position of UAS i that is denoted by $(x_{i,d}, y_{i,d})$ must satisfy

$$\Psi\left(x_{i,d}(t), y_{i,d}(t)\right) = \Psi\left(x_{i,d}(t_0), y_{i,d}(t_0)\right), \quad \forall t \ge t_0,$$
(13)

where t_0 is the initial time at which UAS i joins the airspace.

- 2) **Requirement 2:** We assign Δ as the maximum allowable deviation from the desired path allocated to every UAS.
- 3) **Requirement 3:** The minimum separation distance between two adjacent streamlines $\Psi_i = \Psi\left(x_{i,d}, y_{i,d}\right)$ and $\Psi_j = \Psi\left(x_{j,d}, y_{j,d}\right)$ denoted by l_{ij}^{min} is greater that 2Δ .
- 3) Air Corridor Generation: We decompose the 3-D environment into n_l layers, identified by C_1, \ldots, C_{n_l} , corresponding to different altitudes. Mathematically speaking, $C_i \subset \mathbb{R}^2$ is a horizontal floor parallel to the x-y plane at altitude $z=h_i$.

Let $\mathcal{O}_i^j \subset \mathcal{C}_i$ be the projection of keep-out zone \mathcal{O}_j on \mathcal{C}_i . Using the numerical approach expressed in Section III-A, we can safely exclude $\mathcal{O}_i^1 \bigcup \cdots \mathcal{O}_i^{n_o}$ by obtaining stream function $\Psi_i(x, y)$ over \mathcal{C}_i , and discretize the keep-in space

$$\mathcal{P}_i = \mathcal{C}_i \setminus \left(\mathcal{O}_i^1 \bigcup \cdots \mathcal{O}_i^{n_o}\right), \quad \forall i \in \{1, \dots, n_l\}$$

into a finite number of corridors with the boundaries obtained by level curves with $\Psi_i(x, y) = \text{constant}$, using Eqs. (8a), (8b), and (9).

B. Temporal Planning: Optimal Allocation of Air Corridors to UAS

We define a DP to maximize the usability of the low-altitude airspace through optimal allocations of air corridors to UAS. The DP is defined by tuple (S, A, P, J, γ) with the following elements:

- 1) Finite set of states S;
- 2) Finite set of actions A;
- 3) State transition dynamics defined by tensor

$$P = \bigcup_{s,s' \in \mathcal{S}, a \in \mathcal{A}} P_a(s,s')$$

where $P_a(s, s')$ assigns transition from current state $s \in \mathcal{S}$ to state $s' \in \mathcal{S}$ under action $a \in \mathcal{A}$;

- 4) Cost function idefined by $J: \mathcal{S} \times \mathcal{A} \to \mathbb{R}_+$ where J(s, a) assigns numerical cost at state $s \in \mathcal{S}$ under action $a \in \mathcal{A}$;
- 5) Discount factor $\gamma \in [0, 1]$.

DP value function $V: \mathcal{S} \to \mathbb{R}^+$ defines total expected value corresponding to the sequence of states $s = (s(1), \ldots, s(t), \ldots)$ and actions $a = (a(1), \ldots, a(t), \ldots)$:

$$V = \sum_{t=0}^{\infty} \gamma^t J(s(t), a(t)). \tag{14}$$

Using the value iteration algorithm, we can iterative compute value function $V_i(s): \mathcal{S} \to \mathbb{R}_+$, where subscript i enumerates the number of iterations. In particular, by updating $V_i(s)$ in the following way

$$V_{i+1}(s) = \min_{a} \sum_{s' \in S} P_a(s, s') (J(s, a) + \gamma V_i(s'))$$
 (15)

 $V_i(s)$ converges monotonically and in polynomial time to $V^*(s)$. The threshold ϵ specifies the numerical convergence requirement for value in each state:

$$V^* \approx \min_{s \in S} |V_{i+1}(s) - V_i(s)| \le \epsilon. \tag{16}$$

The optimal policy $\pi^*(s)$ is defined as the sequence of actions that provide the optimal total cost $V^*(s)$ starting at state s and is computed from:

$$\pi^*(s) = \underset{a \in \mathcal{A}}{\operatorname{argmin}} \sum_{s' \in \mathcal{S}} P_a(s, s') (J(s, a) + \gamma V^*(s')). \tag{17}$$

Remark 2: Although, we assume that transitions over the state space are deterministic, we can indirectly incorporate uncertainty into planning by updating the geometry of the keep-out space without changing the dimension of the state space. In other words, if a UAS cannot admit or follow the desired corridor assigned by the authorized decision-maker, it is contained by an keep-out airspace and safely excluded from the keep-in airspace. Note that this problem has been previously investigated by the second and third authors in [35].

Every two points in the desired low-altitude airspace must be "reachable" while UAS coordination safety is ensured. We mandate the same motion direction for all air corridors existing on the same floor in order to assure UTM safety. This requires that at least four floors exist to authorize motions in East, North, West, and South traffic flow directions. Because the air corridors may be already allocated to some UAS who are already using the airspace, without loss of generality, we project the low altitude airspace on eight layers $(n_l = 8)$, denoted by C_1, \dots, C_8 , where:

- Streamlines are elongated along the x axis on C_1 , C_3 , C_5 , and C_7 ;
- Streamlines are elongated along the y axis on C_2 , C_4 , C_6 , and C_8 .

1) DP States: We define \mathcal{L}_i as a finite set identifying the air corridors at $\mathcal{C}_i \subset \mathbb{R}^2$ $(i \in \{1, \dots, 8\})$. Also, we define \mathcal{X} and \mathcal{Y} as finite sets representing discrete values of x and y

coordinates, respectively. The state set $\mathcal S$ is finite and defined by

$$S = \left(\left(\bigcup_{i=1,3,5,7} (\mathcal{L}_i \times \mathcal{X}) \right) \bigcup \left(\bigcup_{i=2,4,6,8} (\mathcal{L}_i \times \mathcal{Y}) \right) \right)$$

where "x" denotes the Cartesian product symbol.

2) *DP Actions:* We specify four possible actions defined by set $A = \{a_1, a_2, a_3, a_4\}$ with the following functionality:

- a_1 : Move forward in the current corridor,
- a_2 : Stay at the current position for the next time,
- a₃: Move to the neighboring higher altitude level,
- a₄: Move to the neighboring lower altitude level.

Remark 3: Because allowable motion directions are the same in all air corridors lying in the same floor, only a_1 can be authorized for a UAS if it does change its altitude.

Note that the actions are constrained to satisfy the following limitations:

- 1) At the highest level a_3 must <u>not</u> be selected.
- 2) At the lowest level a_4 must not be selected.
- 3) Transition from the current state $s \in S$ to the next state $s' \in S$ is allowed only if s' has not already been allocated to another UAS.
- 3) DP State Transition: Because we use a DP model for temporal planning, transitions over the states are deterministic, which in turn implies that probability $P_a(s, s')$ is a binary variable, either 0 or 1 for $a \in \mathcal{A}$ and $s, s' \in \mathcal{S}$. For obtaining the transition probability $P_a(s, s')$, we first define expected next state as follows:

Definition 1: We use $\hat{s}: \mathcal{S} \times \mathcal{A} \to \mathcal{S}$ to define the *expected* next state at every state $s \in \mathcal{S}$ under an action $a \in \mathcal{A}$. Then, the state trasition is defined by

$$P_{a}(s, s') = \begin{cases} 1 & s' = \hat{s}(s, a) \\ 0 & \text{otherwise} \end{cases}, \quad \forall s, s' \in \mathcal{S}, \ \forall a \in \mathcal{A}.$$

$$(18)$$

4) DP Cost: We define subset $S_o \subset S$ as the set of inaccessible states that were already allocated to the existing UAS. Given goal state s_g , as the target destination of the UAS, we define cost J(s, a) as follows:

$$J(s, a) = d(s, s_{\varrho}) + J_0(s, a), \quad \forall s \in \mathcal{S}, \ \forall a \in \mathcal{A}$$
 (19)

where s_g is the final or goal state for a new UAS,

$$d(s, s_g) = \sqrt{(x(s) - x(s_g))^2 + (y(s) - y(s_g))^2 + (z(s) - z(s_g))^2},$$
(20)

is the distance between the next state s' and goal state s_g , where $x(\cdot)$, $y(\cdot)$, and $z(\cdot)$ denote position components of state $s \in \mathcal{S}$, or $s_g \in \mathcal{S}$, and

$$J_0(s, a) = \begin{cases} 10^6 & \hat{s}(s, a) \in \mathcal{S}_o \\ 0 & \text{otherwise.} \end{cases}$$
 (21)

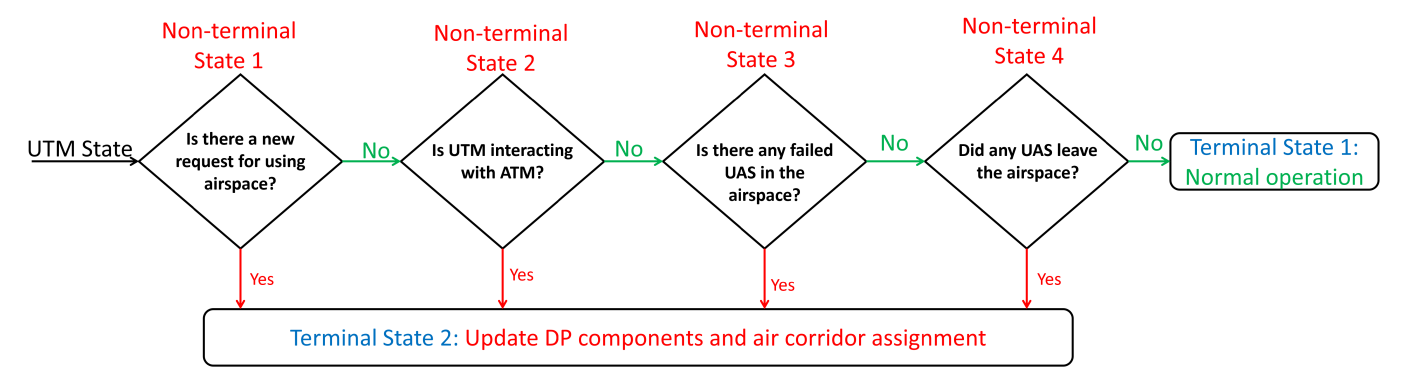


Fig. 3. The state machine used to manage DP updates for safe allocation of UAS to streamline-based airspace corridors.

5) Discount Factor: In this paper, we choose $\gamma = 1$ to optimally assign the air corridors to the UAS. The optimal policy $\pi^*(s)$ obtained by (17) is assigned by the value iteration method.

IV. UTM OPERATION

To safely allocate the airspace to the UAS requesting airspace access, we prioritize the airspace usability by the existing UAS and apply a first-come-first-serve policy to authorize access for the new UAS. Air corridors can be optimally allocated to UAS using the DP approach presented in Section III-B.

Computational cost is reasonable for real-time policy updates because in most air corridors are already assigned to existing UAS inaccessible by updating the DP transitions when there is new request for using the airspace. Therefore, the proposed DP approach assigns airways only to a single UAS after the request is submitted. We apply the state machine shown in Fig. 3 to safely and resiliently implement our proposed UTM system. This state machine consists of two terminal states and four non-terminal states with definitions given in Table I.

Algorithm 1 presents the functionality of our proposed fluid-flow-inspired UTM system. If no non-terminal (NT) state is satisfied, the current policy $\pi^*(s)$ for air corridor allocation is acceptable. If non-terminal (NT) state 2 or NT state 3 is satisfied, we perform the following steps:

- Consider a failed UAS or no-fly zone temporarily allocated to ATM as temporary keep-out airspace, and revise definitions of the air corridors assigned by $\mathcal{L}_1, \dots, \mathcal{L}_8$.
- Update definitions of the state set S, transition probabilities, and cost.
- Update the optimal policy $\pi^*(s)$ by solving Eq. (17).

If NT state 1 or NT state 4 is satisfied, we do not need to revise the state set S and action set A. However, cost and transition functions will change and the updated policy is obtained by solving (17).

V. SIMULATION RESULTS

We consider the example obstacle-laden environment shown in Fig. 4 with a large number of buildings of different lengths, widths, and heights. The motion space is converted into

Algorithm 1 Physics-Inspired UTM System

Input Current UTM state

Input Keep-out airspace \mathcal{O}_1 through \mathcal{O}_{n_o}

Specify air corridors defined by \mathcal{L}_1 through \mathcal{L}_8 .

Define DP components.

Output Assign $\pi^*(s)$ for every $s \in \mathcal{S}$ using Eq. (17).

if \underline{No} non-terminal state is satisfied then

Normal operation

else

if NT state 2 or NT state 3 is satisfied then

Update keep-out airspace zones.

Update air corridors defined by \mathcal{L}_1 through \mathcal{L}_8 .

Update DP state, transitions, and cost.

end if

if NT state 1 or NT state 4 is satisfied then

Update DP cost and transition probabilities.

end if

Obtain optimal policy $\pi^*(s)$ ($\forall s \in \mathcal{S}$) using Eq. (17).

end if

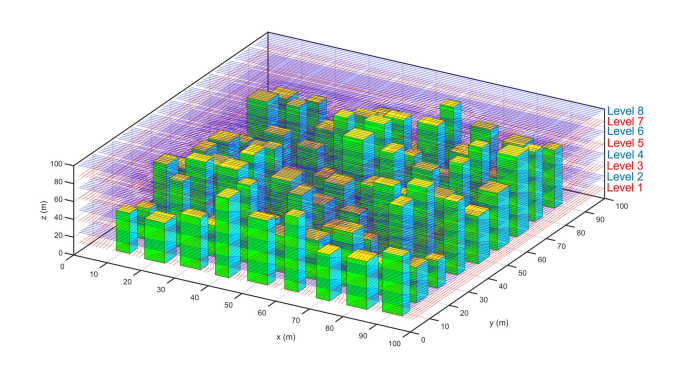


Fig. 4. A virtual urban environment with with a large number of buildings of different lengths, widths, and heights.

 $n_l = 8$ floors at heights z = 12.5m, z = 25m, z = 37.5m, z = 50m, z = 62.5m, z = 75m, z = 87.5m, and z = 100m. By using the proposed spatial planning approach, presented in Section III-A, fixed air corridors at every level are obtained and presented in Fig. 5, where they all safely wrap the obstacles in every level. The red dots sown in Fig. 5 represents locations that allocated to other UAS, and thus, cannot be accessed by a new UAS requesting to use the airspace. For the temporal planning, the state space is 91×91 grid, therefore,

TABLE I
TERMINAL AND NON-TERMINAL STATES OF THE STATE MACHINE USED FOR TO MANAGE OPTIMAL UAS AIR CORRIDOR ALLOCATION

	Implication
Terminal State 1	Normal Operation: Current optimal allocation of air corridors are acceptable.
Terminal State 2	Update definitions of states, actions, transition probabilities, and cost; update the air corridor assignment.
Non-Terminal State 1	Check if the UTM interfaces with ATM.
Non-Terminal State 2	Check if there is a new request for entering or departing the airspace.
Non-Terminal State 3	Check if there are any failed UAS in the airspace.
Non-Terminal State 4	Check if there is a new request for entering or departing the airspace.

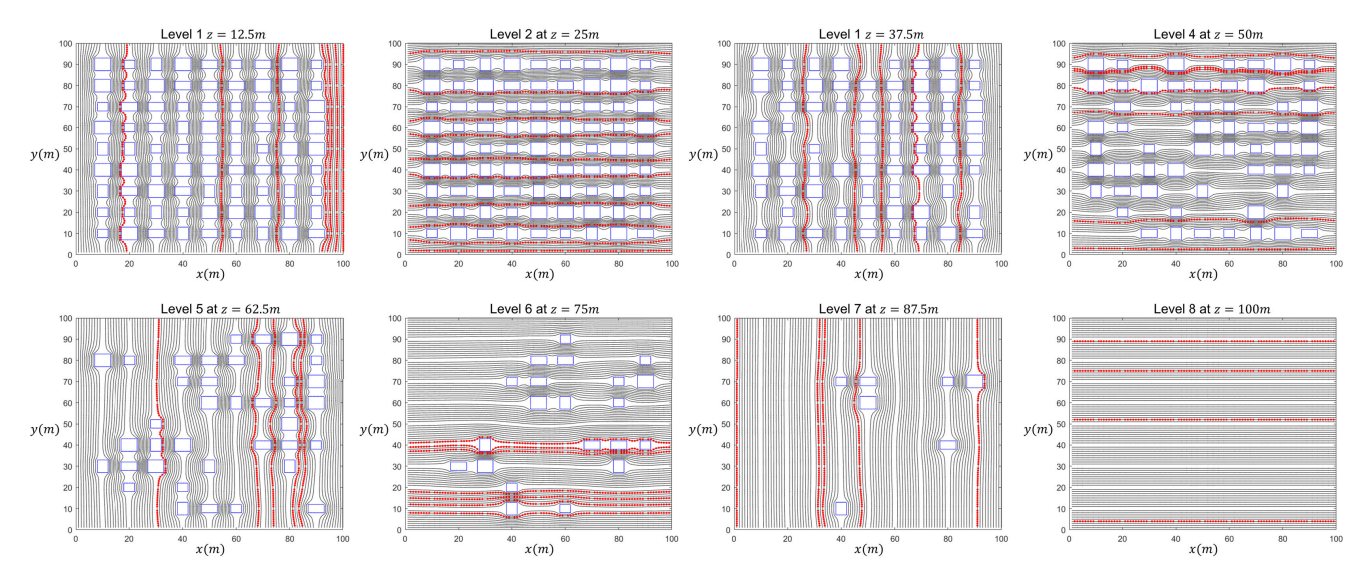


Fig. 5. Fixed air corridors, at levels \mathcal{L}_1 through \mathcal{L}_8 , are obtained by the proposed spatial planning approach presented in Section III-A. As illustrated, they all safely wrap the obstacles. The red spots are the locations currently allocated to other UAS, thus, they cannot be accessed by the new UAS requesting to use the airspace.

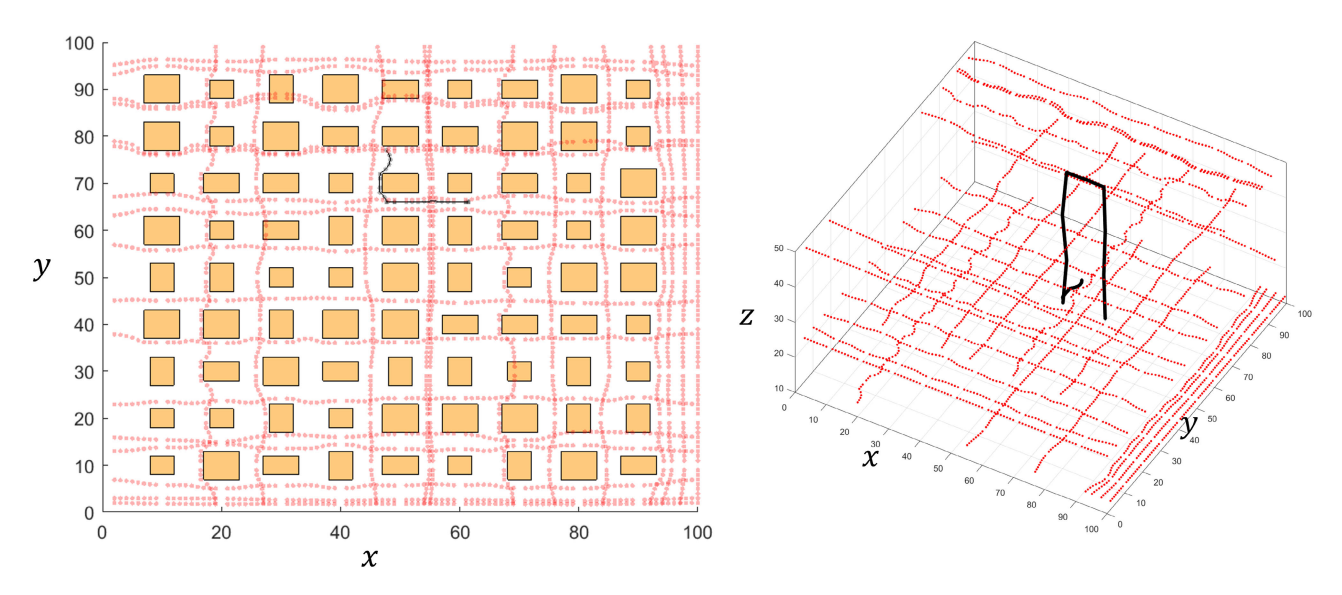


Fig. 6. Optimal path allocated to the new UAS: (Left) Top viw of the airspace with optimal path of the new UAS shown by black. (right) Optimal path of the new UAS in a 3-D motion space.

Time	1	2	3	4	5	6	7	8	9	10	11	12	13	14	15	16	17	18	19	20	21	21	21	24	25	26
Forward																										
Up																										
Down																										

Fig. 7. The optimal actions of the new UAS to reach from $(x_0, y_0, z_0) = (61.4510, 66, 12.5)$ to $(x_f, y_f, z_f) = (47.5973, 77, 12.5)$.

 $|\mathcal{S}| = 66248$ is the cardinality of the state set \mathcal{S} . The optimal policy, assigned by using value iteration method, is obtained by 140 iterations.

We consider a scenario at which one UAS requests to join the airspace at initial position $(x_0, y_0, z_0) = (61.4510, 66, 12.5)$ and reaches the final position $(x_f, y_f, z_f) = (47.5973, 77, 12.5)$. The optimal path allocated to this UAS is obtained by using the temporal panning method presented in Section III-B, and shown in Fig. 6. For the given initial and final positions, the optimal actions are obtained by solving the bellman equations and presented in the Table of Fig. 7.

VI. CONCLUSION

This paper has proposed and utilized a novel fluid-flow-based method to safely manage low altitude UAS traffic in low-altitude airspace over a potentially complex urban environment. We used the fundamentals of Eulerian continuum mechanics to spatially define airway corridors around obstacles wrapping buildings and restricted flight zones at low-altitude airspace.

By using this continuum-mechanics-based solution, we showed that we can generate fixed air corridors at low-altitude airspace where they safely wrap buildings to provide obstacle-free paths. By using the principles of the Eulerian continuum mechanics, we treated UAS coordination as an ideal fluid flow with stream and potential functions that are governed by the Laplace PDE. As a result, we defined air corridors as the streamlines of fluid flow pattern, and contributed a method for assigning conditions on the stream conditions over the external boundaries of the obstacles and the motion space, allowing for the passage of air corridors through tight spaces between buildings in low altitude airspace.

For the temporal planning, we developed a DP to optimally plan transitions over the airspace, and therefore, efficiently allocate space and time to UAS. Because air corridors already assigned to existing UAS become inaccessible, after a new request request is made, the DP-based method needs to assign air corridor only to one UAS. As a result the proposed management system offers scalability, and supports airspace usability maximization. The efficacy of the proposed method was shown in simulation for a highly obstacle-laden environment.

In future work, we will explore temporal planning in the presence of uncertainty, where we will replace the proposed DP by a Markov Decision Processes (MDP) model to optimally assign transitions over the fixed air corridors at low altitude airspace. We envision that the uncertainty must be incorporated in modeling to capture dynamic environmental and weather conditions as well as incomplete knowledge of other UAS intentions. We will apply reinforcement learning models to consistently learn transition probabilities and incorporate them into UTM.

REFERENCES

[1] L. R. Newcome, Unmanned Aviation: A Brief History of Unmanned Aerial Vehicles. Reston, VA, USA: AIAA, 2004.

- [2] S. Jung and K. Hyunsu, "Analysis of Amazon prime air UAV delivery service," J. Knowl. Inf. Technol. Syst., vol. 12, no. 2, pp. 253–266, Apr. 2017.
- [3] B. Argrow, D. Lawrence, and E. Rasmussen, "UAV systems for sensor dispersal, telemetry, and visualization in hazardous environments," in Proc. 43rd AIAA Aerosp. Sci. Meeting Exhibit, Jan. 2005, p. 1237.
- [4] D. C. Tsouros, S. Bibi, and P. G. Sarigiannidis, "A review on UAV-based applications for precision agriculture," *Information*, vol. 10, no. 11, p. 349, Nov. 2019.
- [5] E. Semsch, M. Jakob, D. Pavlicek, and M. Pechoucek, "Autonomous UAV surveillance in complex urban environments," in *Proc. IEEE/WIC/ACM Int. Joint Conf. Web Intell. Intell. Agent Technol.*, vol. 2, Sep. 2009, pp. 82–85.
- [6] H. Surmann et al., "Integration of UAVs in urban search and rescue missions," in *Proc. IEEE Int. Symp. Saf., Secur., Rescue Robot. (SSRR)*, Sep. 2019, pp. 203–209.
- [7] J. Witczuk, S. Pagacz, A. Zmarz, and M. Cypel, "Exploring the feasibility of unmanned aerial vehicles and thermal imaging for ungulate surveys in forests-preliminary results," *Int. J. Remote Sens.*, vol. 39, nos. 15–16, pp. 5504–5521, Aug. 2018.
- [8] E. V. Butilă and R. G. Boboc, "Urban traffic monitoring and analysis using unmanned aerial vehicles (UAVs): A systematic literature review," *Remote Sens.*, vol. 14, no. 3, p. 620, Jan. 2022.
- [9] B. Sridhar, K. S. Sheth, and S. Grabbe, "Airspace complexity and its application in air traffic management," in *Proc. 2nd USA/Europe Air Traffic Manage R&D Seminar*. Washington, DC, USA: Federal Aviation Administration, 1998, pp. 1–6.
- [10] T. Prevot, J. Rios, P. Kopardekar, J. E. Robinson, III, M. Johnson, and J. Jung, "UAS traffic management (UTM) concept of operations to safely enable low altitude flight operations," in *Proc. 16th AIAA Aviation Technol.*, *Integr., Oper. Conf.*, Jun. 2016, p. 3292.
- [11] J. Rios, D. Mulfinger, J. Homola, and P. Venkatesan, "NASA UAS traffic management national campaign: Operations across six UAS test sites," in *Proc. IEEE/AIAA 35th Digit. Avionics Syst. Conf. (DASC)*, Sep. 2016, pp. 1–6.
- [12] P. Kopardekar, J. Rios, T. Prevot, M. Johnson, J. Jung, and J. E. Robinson, "Unmanned aircraft system traffic management (UTM) concept of operations," in *Proc. AIAA Aviation Aeronaut. Forum (Aviation)*, 2016, pp. 1–16.
- [13] T. Jiang, J. Geller, D. Ni, and J. Collura, "Unmanned aircraft system traffic management: Concept of operation and system architecture," *Int. J. Transp. Sci. Technol.*, vol. 5, no. 3, pp. 123–135, Oct. 2016.
- [14] E. Sunil et al., "Metropolis: Relating airspace structure and capacity for extreme traffic densities," in *Proc. 11th USA/Eur. Air Traffic Manage.* Res. Develop. Seminar (ATM), Lisbon, Portugal, Jun. 2015, pp. 1–11.
- [15] J. Lundberg, K. L. Palmerius, and B. Josefsson, "Urban air traffic management (UTM) implementation in cities—Sampled side-effects," in *Proc. IEEE/AIAA 37th Digit. Avionics Syst. Conf. (DASC)*, Sep. 2018, pp. 1–7.
- [16] A.-Q. V. Dao et al., "Evaluation of early ground control station configurations for interacting with a UAS traffic management (UTM) system," in *Advances in Human Factors in Robots and Unmanned Systems* (Advances in Intelligent Systems and Computing), vol. 595, J. Chen, Eds. Cham, Switzerland: Springer, 2018. [Online]. Available: https://link.springer.com/chapter/10.1007/978-3-319-60384-1_8, doi: 10.1007/978-3-319-60384-1_8.
- [17] Revising the Airspace Model for the Safe Integration of Small Unmanned Aircraft Systems, Amazon Prime Air, Washington, DC, USA, 2015.
- [18] V. Battiste, A.-Q.-V. Dao, T. Z. Strybel, A. Boudreau, and Y. K. Wong, "Function allocation strategies for the unmanned aircraft system traffic management (UTM) system, and their impact on skills and training requirements for UTM operators," *IFAC-PapersOnLine*, vol. 49, no. 19, pp. 42–47, 2016.
- [19] C. A. Ochoa and E. M. Atkins, "Urban metric maps for small unmanned aircraft systems motion planning," *J. Aerosp. Inf. Syst.*, vol. 19, no. 1, pp. 37–52, 2022.
- [20] D. Feng, P. Du, H. Shen, and Z. Liu, "UAS traffic management in low-altitude airspace based on three dimensional digital aerial corridor system," in *Urban Intelligence and Applications* (Studies in Distributed Intelligence), X. Yuan and M. Elhoseny, Eds. Cham, Switzerland: Springer, 2020. [Online]. Available: https://link.springer.com/chapter/10.1007/978-3-030-45099-1_14, doi: 10.1007/978-3-030-45099-1_14.

- [21] W. Zhai, B. Han, D. Li, J. Duan, and C. Cheng, "A low-altitude public air route network for UAV management constructed by global subdivision grids," *PLoS ONE*, vol. 16, no. 4, Apr. 2021, Art. no. e0249680.
- [22] M. Stevens and E. Atkins, "Geofence definition and deconfliction for UAS traffic management," *IEEE Trans. Intell. Transp. Syst.*, vol. 22, no. 9, pp. 5880–5889, Sep. 2021.
- [23] M. N. Stevens, H. Rastgoftar, and E. M. Atkins, "Geofence boundary violation detection in 3D using triangle weight characterization with adjacency," J. Intell. Robot. Syst., vol. 95, no. 1, pp. 239–250, Jul. 2019.
- [24] M. N. Stevens, H. Rastgoftar, and E. M. Atkins, "Specification and evaluation of geofence boundary violation detection algorithms," in *Proc. Int. Conf. Unmanned Aircr. Syst. (ICUAS)*, Jun. 2017, pp. 1588–1596.
- [25] J. Kim and E. Atkins, "Airspace geofencing and flight planning for lowaltitude, urban, small unmanned aircraft systems," *Appl. Sci.*, vol. 12, no. 2, p. 576, 2022.
- [26] F. Duchoň et al., "Path planning with modified a star algorithm for a mobile robot," *Proc. Eng.*, vol. 96, pp. 59–69, Jan. 2014.
- [27] A. Stentz, "Optimal and efficient path planning for partially-known environments," in *Proc. IEEE Int. Conf. Robot. Automat.* San Diego CA, USA: IEEE, 1994, pp. 3310–3317.
- [28] B. Burns and O. Brock, "Sampling-based motion planning using predictive models," in *Proc. IEEE Int. Conf. Robot. Autom.*, Apr. 2005, pp. 3120–3125.
- [29] I. Noreen, A. Khan, and Z. Habib, "Optimal path planning using RRT* based approaches: A survey and future directions," *Int. J. Adv. Comput. Sci. Appl.*, vol. 7, no. 11, pp. 97–107, 2016.
- [30] H. Liu, G. Xie, and L. Wang, "Necessary and sufficient conditions for containment control of networked multi-agent systems," *Automatica*, vol. 48, no. 7, pp. 1415–1422, 2012.
- [31] W. Ren, R. W. Beard, and E. M. Atkins, "A survey of consensus problems in multi-agent coordination," in *Proc.*, *Amer. Control Conf.*, 2005, pp. 1859–1864.
- [32] J. Kim, K.-D. Kim, V. Natarajan, S. D. Kelly, and J. Bentsman, "PdE-based model reference adaptive control of uncertain heterogeneous multiagent networks," *Nonlinear Anal., Hybrid Syst.*, vol. 2, no. 4, pp. 1152–1167, Nov. 2008.
- [33] L. Wang and Q. Guo, "Distance-based formation stabilization and flocking control for distributed multi-agent systems," in *Proc. IEEE Int. Conf. Mechatronics Autom. (ICMA)*, Aug. 2018, pp. 1580–1585.
- [34] H. Rastgoftar and E. M. Atkins, "Continuum deformation of multi-agent systems under directed communication topologies," J. Dyn. Syst., Meas., Control, vol. 139, no. 1, Jan. 2017, Art. no. 011002.
- [35] H. Rastgoftar and E. Atkins, "Physics-based freely scalable continuum deformation for UAS traffic coordination," *IEEE Trans. Control Netw. Syst.*, vol. 7, no. 2, pp. 532–544, Jun. 2020.
- [36] H. Uppaluru, H. Emadi, and H. Rastgoftar, "Resilient multi-UAS coordination using cooperative localization," *Aerosp. Sci. Technol.*, vol. 131, p. 107960, 2022.
- [37] H. Emadi, H. Uppaluru, and H. Rastgoftar, "A physics-based safety recovery approach for fault-resilient multi-quadcopter coordination," in *Proc. Amer. Control Conf. (ACC)*. IEEE, 2022, pp. 2527–2532.
- [38] L. Wang, A. D. Ames, and M. Egerstedt, "Safety barrier certificates for collisions-free multirobot systems," *IEEE Trans. Robot.*, vol. 33, no. 3, pp. 661–674, Jun. 2017.
- [39] A. D. Ames, S. Coogan, M. Egerstedt, G. Notomista, K. Sreenath, and P. Tabuada, "Control barrier functions: Theory and applications," in *Proc. 18th Eur. Control Conf. (ECC)*, Jun. 2019, pp. 3420–3431.
- [40] A. D. Ames, J. W. Grizzle, and P. Tabuada, "Control barrier function based quadratic programs with application to adaptive cruise control," in *Proc. 53rd IEEE Conf. Decis. Control*, Dec. 2014, pp. 6271–6278.
- [41] P. D. Vascik, J. Cho, V. Bulusu, and V. Polishchuk, "Geometric approach towards airspace assessment for emerging operations," *J. Air Transp.*, vol. 28, no. 3, pp. 124–133, Jul. 2020.

- [42] M. Jankovic, "Robust control barrier functions for constrained stabilization of nonlinear systems," *Automatica*, vol. 96, pp. 359–367, Oct 2018
- [43] Y. Chen, A. Singletary, and A. D. Ames, "Guaranteed obstacle avoidance for multi-robot operations with limited actuation: A control barrier function approach," *IEEE Control Syst. Lett.*, vol. 5, no. 1, pp. 127–132, Jan. 2021.
- [44] H. Rastgoftar, "Fault-resilient continuum deformation coordination," IEEE Trans. Control Netw. Syst., vol. 8, no. 1, pp. 423–436, Mar. 2021.
- [45] J. J. P. Veerman and R. Lyons, "A primer on Laplacian dynamics in directed graphs," 2020, arXiv:2002.02605.



Hossein Rastgoftar (Member, IEEE) received the B.Sc. degree in mechanical engineering-thermofluids from Shiraz University, Shiraz, Iran, the joint M.S. degree in mechanical systems and solid mechanics from Shiraz University and the University of Central Florida, Orlando, FL, USA, and the Ph.D. degree in mechanical engineering from Drexel University, Philadelphia, in 2015. He is currently an Assistant Professor with the Department of Aerospace and Mechanical Engineering, The University of Arizona, and an Adjunct Assistant

Professor with the Department of Aerospace Engineering, University of Michigan, Ann Arbor.



Hamid Emadi received the B.Sc. degree in mechanical engineering and the M.S. degree in mechanical systems and solid mechanics from Shiraz University, Shiraz, Iran, and the Ph.D. degree in mechanical engineering from Iowa State University, Ames, IA, USA, in 2021. He was a Post-Doctoral Research Associate with the Dr. Rastgoftar's Group, Department of Aerospace and Mechanical Engineering, The University of Arizona, Tucson, AZ, USA. His research interests include decision making, game theory, optimization, and control.



Ella M. Atkins (Senior Member, IEEE) received the B.S. and M.S. degrees in aeronautics and astronautics from MIT and the M.S. and Ph.D. degrees in computer science and engineering from the University of Michigan. She is currently a Fred D. Durham Professor and the Head of the Kevin T. Crofton Aerospace and Ocean Engineering Department, Virginia Tech. Previously, she was a Professor with the Department of Aerospace Engineering and the Department of Robotics, University of Michigan. She is an AIAA Fellow and a Private Pilot. She

served on the National Academy's Aeronautics and Space Engineering Board. She has authored over 230 refereed journals and conference papers. She is an Editor of the AIAA Journal of Aerospace Information Systems.